Lecture 7
Physical Processes for Diffuse Interstellar Gas

1. Background
2. Cooling Processes
3. Heating Processes
4. Ionization

Appendix A. O+ + H Charge Exchange

Appendix B. Dielectronic Recombination

References

Tielens, Chs. 2-3
Dopita & Sutherland, Chs. 5-7
Lecure04 (introduction to heating and cooling)

1. Background

So far we have discussed:

1. absorption lines, which probe cool neutral gas in nearby diffuse & translucent clouds

2. ***emission lines*** generated by hot ionized gas in HII regions

3. ***continuum extinction and emission*** by dust and the properties of grains and large molecules

We used of simplified models, such as uniform slabs (for clouds) and spheres (for HII regions) to introduce some of the microphysical processes that operate in the ISM.

Background (cont'd)

We now broaden the discussion in order to deal with the *global properties* of the diffuse ISM.
As emphasized in Lecture 01, the physical conditions of the ISM are extraordinarily diverse, with wide ranges for the parameters,

$$n_{\rm H} \sim 10^{-3} - 10^{6} {\rm cm}^{-3}$$
$$T \sim 10 - 10^{6}\ {\rm K}$$
$$x_{\rm e} \sim 0 - 1$$

Consequently, the physical processes also have a wide range, and the previous discussion of atomic processes must be broadened.

The Phases

We have used a simple *ionization classification* based on hydrogen: HI and HII. It is common but not universal to bring some order into the wide range of conditions in the ISM by introducing a

temperature-ionization classification scheme

effected by "multiplying" a *T*-letter (H = hot, W = warm, and C = cool) by an ionization letter *(I* = fully ionized and N= partially ionized) to get four "phases".

Temperature	Ionization	Phase
H ($>10^5$ K)	I	HIM
W (10^2-10^4 K)	I	WIM
W (10^2-10^4 K)	N	WNM
C ($<10^2$ K)	N	CNM

2. Cooling

Recall from Lecture 4: To solve the heat equation for *T*,

$$\rho T \frac{ds}{dT} = \Gamma - \Lambda$$

we need the heating and cooling functions *Γ* and *Λ*. The cooling function is

$$\Lambda = \sum_{ul} n_c (n_l k_{lu} - n_u k_{ul}) E_{ul} = \sum_{ul} \beta_{ul} A_{ul} n_u E_{ul}$$

The second form contains the ***escape probability*** β_{ul}, mentioned earlier with little discussion. It is based on the idea that a cooling photon is either absorbed locally or escapes the region. Here it is best to start from the *total cooling* of the region of concern (its line luminosity),

$$L = \int dV \, \Lambda = A_{ul} h\nu_{ul} \int dV n_u \left\langle \frac{1 - e^{-\tau_{ul}}}{\tau_{ul}} \right\rangle = N_u A_{ul} h\nu_{ul} \beta_{ul}$$

where N_u is the total number of atoms in the volume.

Escape Probability

In this approximation, the escape probability is an average over the source volume and over all directions of the *local escape function* at each location, and a truly global property of the region.

$$\beta_{ul} = \frac{1}{N_u} \int dV \; n_u \left\langle \frac{1 - e^{-\tau_{ul}}}{\tau_{ul}} \right\rangle$$

The choice of the *local escape function* as $(1 - e^{-\tau_{ul}})/\tau_{ul}$ is still arbitrary, but it reproduces exact results in many cases. At least this function has the correct limits in the limit $\tau \rightarrow 0$ and infinity, which are 1 and zero (as $1/\tau$). Our previous use of β in the local cooling function (previous slide) is a further approximation.

For additional discussion of the escape probability, see the 2006 Lecture 11 by JRG, and the the references cited there as well as Tielens Sec. 2.3.2, Shu I Ch. 9 and Osterbrock/Ferland Sec. 4.5

Two-Level Cooling Function

Next recall from Lecture 4 the two-level cooling rate

$$\Lambda_{ul} = \beta_{ul} A_{ul} n_u E_{ul} \frac{(g_u / g_l) e^{-E_{ul}/kT}}{1 + (g_u / g_l) e^{-E_{ul}/kT} + n_{crit} / n_c}$$

$$n_{\rm crit} = \frac{\beta_{ul} A_{ul}}{k_{ul}}$$

which has the low-density ($\beta = 1$) limit

$$\Lambda_{ul} = \lambda_{ul} n_H^{\ 2}$$

$$\lambda_{ul} = x_c x (\frac{g_u}{g_l}) k_{ul}(T) \exp(-T_{ul}/T) k_B T_{ul}$$

where x = abundance of the line coolant. x_c= abundance of the collision partner and $T_{ul} = E_{ul} / k_B$. The ***critical density*** indicates when the low-density limit is applies. It is determined by the *collisional rate coefficient* $k_{ul.}$, which is often poorly known. Notice how the escape probability affects the critical density.

Atomic Cross Sections

1. Cross sections and rate coefficients

The critical density $n_{\rm crit} = A_{ul}/k_{ul}$ depends on the de-excitation rate coefficient, which is related to the excitation rate coefficient by detailed balance

$$k_{lu} = (g_u/g_l)e^{-E_{ul}/kT}k_{ul}$$

A rate coefficient is a thermal average of a cross section e.g.,

$$k_{ul} = \left\langle \sigma_{ul}(v)v \right\rangle = (m/2\pi kT)^{3/2} 4\pi \int_{-\infty}^{\infty} dv v^3 e^{-(1/2)mv^2/kT}\sigma_{ul}(v)$$

Introducing the c.m. energy, E = 1/2 mv^2, instead of the relative speed v, this becomes

$$k_{ul} = \left\langle v(T) \right\rangle \frac{1}{(kT)^2}\int_{-\infty}^{\infty} dE E e^{-E/kT}\sigma_{ul}(E), \qquad \left\langle v \right\rangle = \sqrt{\frac{8}{\pi}\frac{kT}{\mu}}$$

where <v> is the mean speed and μ is the reduced mass.

For a constant cross section, $k_{ul} \propto \langle v \rangle \propto T^{1/2}$, whereas for a Coulomb interaction, where the cross section depends on 1/E (Jackson Eq. 13.104), $k_{ul} \propto T^{-1/2}$.

Atomic Cross Sections (cont'd)

2. Orders of magnitude - Atomic radii *a* are ~ Å, and the *geometric cross section* is $\sigma_{\rm geom} = \pi a^2 \approx 3{\rm x}10^{-16}$ cm^2. Cross sections can be much larger or much smaller, depending on the interaction between projectile and target.

- **Photon interactions** are weaker than those for particles by the factor $\alpha \approx 1/137$, so the standard unit is 1μb = 10^{-18} cm^2, where 1 barn (b) is the nuclear unit 10^{-24} cm^2.
- **Particle reactions** depend strongly on the long-range nature of the interaction potential, especially at low energies, since they determine the particle trajectories before and after collision.
  - -- 1/r **Coulomb**, e.g., electronic excitation of ions (e+ + A^+)
  - -- $1/r^4$ **polarization potential**, e.g. excitation via e + A and H + A^+
  - -- $1/r^6$ **van der Waals** potential, e.g., neutral excitation H + A

NB The $1/r^4$ potential arises from the ion inducing a dipole in the neutral and then interacting with it. The $1/r^6$ potential is the interaction between the two induced dipoles of the neutrals associated with their quantum mechanical zero-point motion.

Atomic Cross Sections (cont'd)

The three main long range potentials lead to cross sections that depend on power laws in velocity and temperature, recalling that

$$k_{ul} = \langle v(T) \rangle \frac{1}{(kT)^2} \int_{-\infty}^{\infty} dE E e^{-E/kT} \sigma_{ul}(E)$$

Interaction	cross section	rate coefficient	magnitude[a]
1/r **Coulomb**	v^{-2}	$T^{-1/2}$	10^{-7} b
$1/r^4$ **polarization**	v^{-1}	T^{0}	10^{-9}
$1/r^6$ **van der Waals**	$v^{-2/3}$	$T^{1/6}$	10^{-11}

a. Rough order of magnitude in $cm^3 s^{-1}$
b. Based on $T=10^4$ K

Cross sections can also depend on the short-range part of the interaction, especially for reactions with neutral particles and at intermediate energies (~1eV). For more details, see Tielens Sec. 4.1, especially for applications to molecules and chemical reactions.

Atomic Cross Sections (cont'd)

3. Electron Collisional Rates - In Lecture 03, we quoted the standard form for the electronic collisional de-excitation rates of the levels of atomic ions and atoms

$$k_{ul} = \frac{8.629 \mathrm{x} 10^{-6}}{T^{1/2}} \frac{\Omega_{ul}}{g_u}$$

For electron-ion collisions, the collision strength Ω_{ul} is approximately constant and of order unity for ions with unit charge, increasing as the charge increases. This formula is also applied to electronic de-excitation of neutral atoms. In his case, Ω_{ul} has to increase with temperature to cancel the $T^{-1/2}$ in the denominator, since the rate coefficient does not have this dependence characteristic of a pure Coulomb interaction.

NB Much less is known about neutral excitation of atoms, e.g., by H, He and H_2.

Optically Thin Low-Density Cooling Curve

OVI etc.

H lines

Forbidden lines

Fine-structure transitions

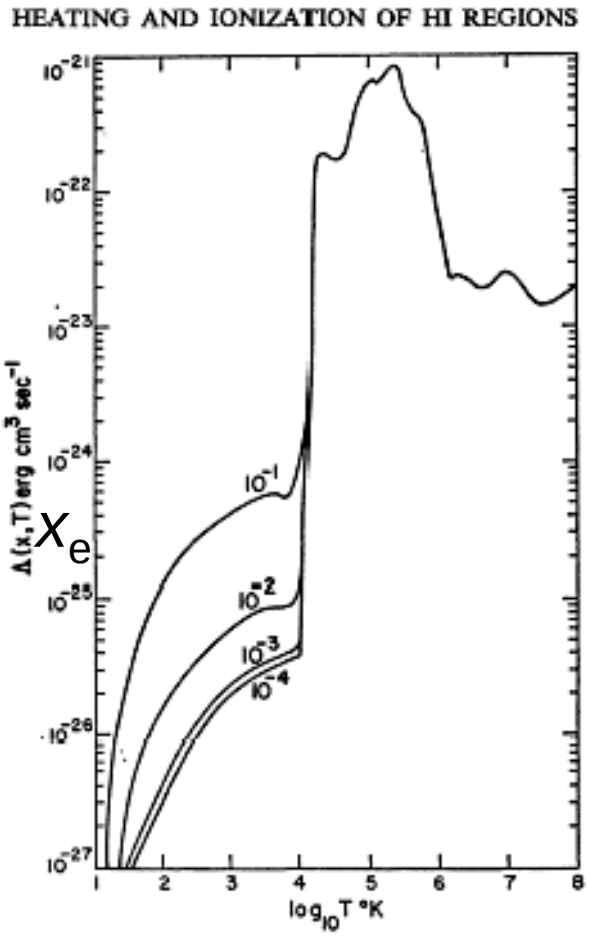

Fe ions

Bremsstrahlung

$\lambda_{ul} = \Lambda_{ul} / n_H^{\,2}$ plotted vs. T (c.f. slide 7)

Dalgarno & McCray, ARAA 10 375 1972
(now out of date)

Optically Thin Low-Density Cooling Curve

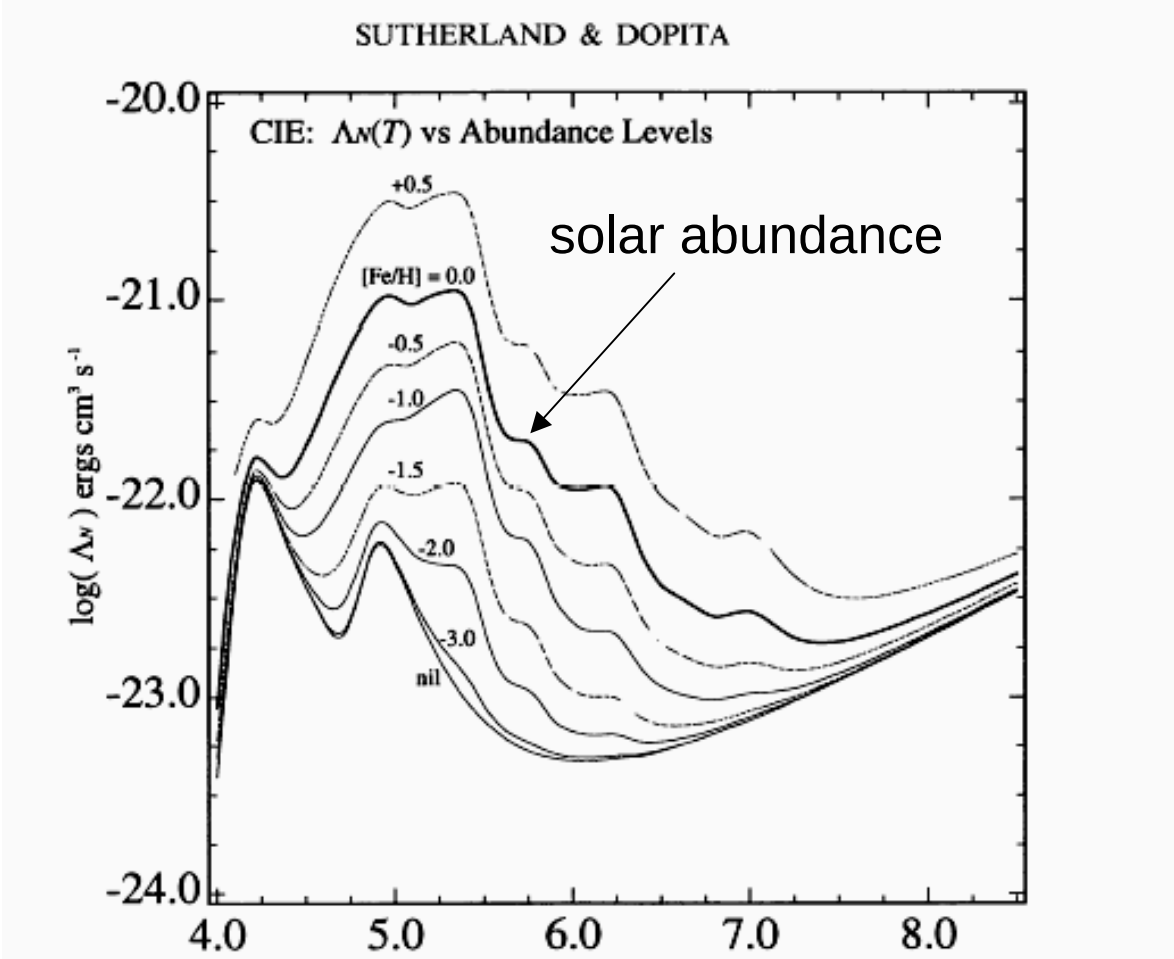

Sutherland & Dopita, ApJ 88, 253, 1993. Cooling curve for $T > 10^4$K and varying metallicity (Fe abundance)

Low Temperature Atomic Coolants

With increasing *T*, a succession of atomic coolants dominates the cooling curve. As discussed in Lecture 04, forbidden transition are important around *T* = 10,000K. At lower temperatures, characteristic of the cool phases of the diffuse gas (c.f., slide 4), atomic *fine-structure lines* become important. If the gas is shielded from UV radiation,molecules can form, but we postpone molecular cooling until Part II of this course.

Low-lying fine-structure cooling lines are generated by abundant ions whose ground states have finite spin and finite orbital angular momenta, especially

$$\mathrm{CI}\ (^3\mathrm{P}),\ \mathrm{CII}\ (^2\mathrm{P}),\ \mathrm{OI}\ (^3\mathrm{P})$$

We might also consider NII (^{3}P), except that nitrogen is mainly in NI, and Si(^{3}P), SiII (^{2}P), FeI (^{5}D) & FeII (^{6}D), except that Si and Fe are strongly depleted in dust grains. However, SI(^{3}P) May play a role since it is not depleted very much.

Important Fine-Structure Coolants

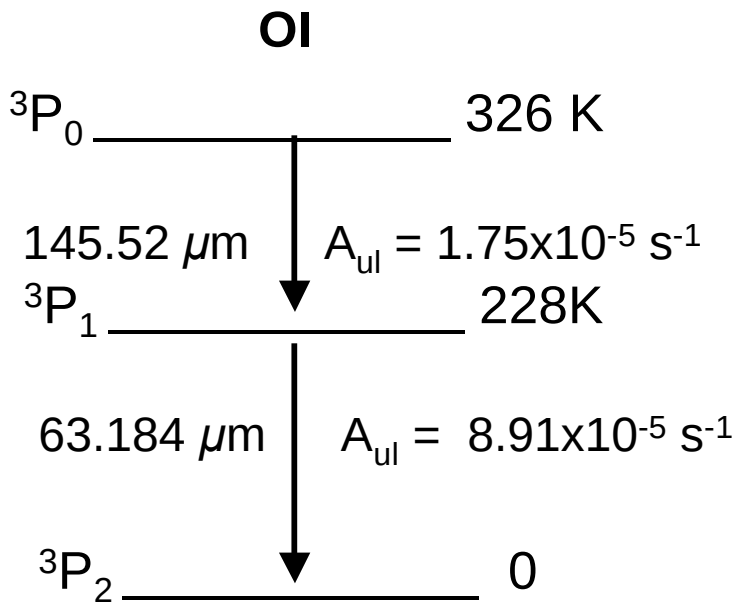

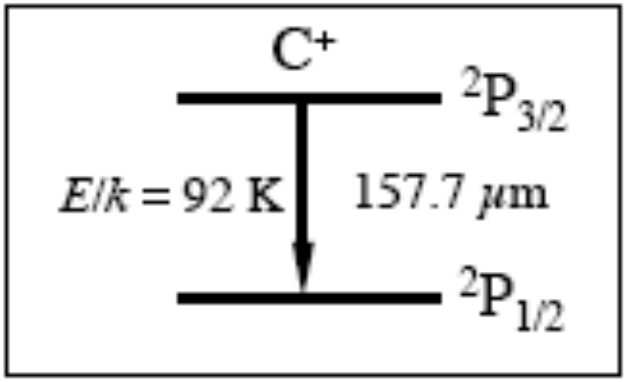

A_{ul} = 2.29x10^{-6} s^{-1}

The CII 158 micron line is the strongest line in the FIR emission of the Milky Way

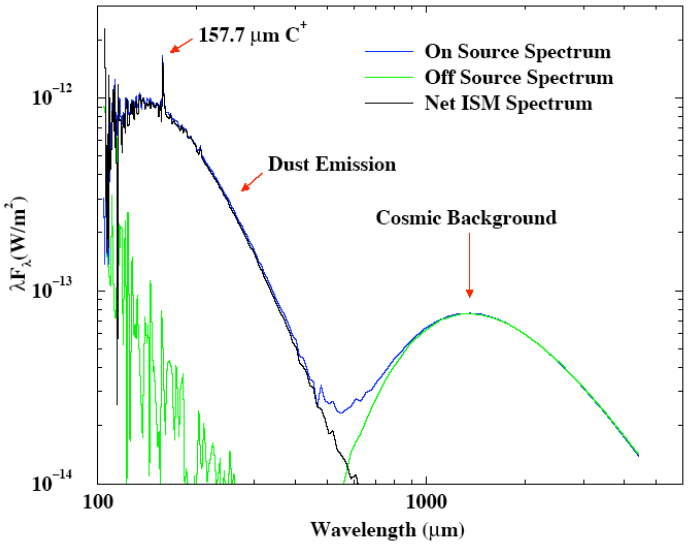

Estimate of CII Fine-Structure Cooling

The low-density two-level formula applies in this case

$$\Lambda_{ul} = \lambda_{ul} n_H{}^2 \qquad \lambda_{ul} = x_c x(\frac{g_u}{g_l}) k_{ul}(T) \exp(-T_{ul}/T) k_B T_{ul}$$

with x=x(H)=1 and c = e and H. The collisional de-excitation rate coeff0cients are:

$$k_{ul}^{\mathrm{H}} = 3.75\mathrm{x}10^{-11}\ T^{0.15}\mathrm{cm}^3\mathrm{s}^{-1} \quad \text{(Barinovs et al. ApJ, 620, 537, 2005)}$$

$$\Omega_{ul}{}^{\mathrm{e}} \cong 1.8 \quad \text{or} \quad k_{ul}{}^{\mathrm{e}} \cong 3.9\mathrm{x}10^{-06}\ T^{-1/2}\ \mathrm{cm}^3\mathrm{s}^{-1}$$

(Wilson & Bell, MNRAS, 337, 1027, 2002), or

$$k_{ul}{}^{\mathrm{e}} / k_{ul}^{\mathrm{H}} = 1.04\mathrm{x}10^4\, T^{-0.65}, \text{ and}$$

$$\lambda_{ul} = 9.4\mathrm{x}10^{-28} \left[\frac{x(\mathrm{C}^+)}{10^{-4}}\right] (1 + \frac{1.04\mathrm{x}10^4}{T^{0.65}} x_{\mathrm{e}}) T^{0.15} e^{-91.211/T}\ \mathrm{erg\ cm}^3\mathrm{s}^{-1}$$

This quantity must still be multiplied by $n_{\mathrm{H}}{}^2$ to obtain the cooling rate per unit volume.

3. Heating

Unlike line cooling, which is reasonably well understood (despite our ignorance of collisional rate coefficients), it is impossible to give a general treatment of heating. From Lecture 04, we recall the general categories of heating:

1. Radiative (UV through X-ray bands)
2. Cosmic rays
3. Collisions with warm dust
4. Dissipation of mechanical energy (stellar winds, SNRs, shocks, turbulence)
5. Magnetic forces (reconnection & ambipolar diffusion).

Each of these requires a detailed analysis of the energy source and the energy-dissipation process. Here we discuss only the first two.

Cosmic Ray Ionization and Heating

We postpone a detailed discussion of this topic until later, starting with Lecture 09 (Cosmic Rays and Magnetic Fields). Here we merely quote the rate in terms of the ionization rate ζ_{CR} per H nucleus and measure it in units of 10^{-17} s^{-1}. The ionizations rate per unit volume is then

$$\left.\frac{dn}{dt}\right|_{CR} = \zeta_{CR}\, n_H \qquad \Gamma_{CR} = \zeta_{CR}\, n_H \Delta E_{CR}$$

With typical values for atomic regions,

$$\zeta_{CR} = 10^{-17}\, s^{-1} \qquad \Delta E_{CR} = 7\mathrm{eV}$$

the heating rate per unit volume is

$$\Gamma_{CR} = 1.12\mathrm{x}10^{-28}\left(\frac{\zeta_{CR}}{10^{-17}\, s^{-1}}\right)\left(\frac{\Delta E_{CR}}{7\mathrm{eV}}\right) n_H \ \mathrm{erg\ cm^{-3}\ s^{-1}}$$

Photoelectric Heating in Neutral Regions

The most energetic radiation in neutral regions c.f. FUV photons longward of the Lyman limit (911.6 Å or 13.6 eV). Except for the rare gases, oxygen and nitrogen, most abundant cosmic elements have first Ionization Potentials IP < 13.6 eV (c.f. Table, next slide). Thus, unlike HII regions, the targets for photoelectric heating are limited to carbon and perhaps sulfur, since Si, Mg, and Fe tend to be depleted in dust, Lec05). Here we treat the case of carbon.

Unlike the treatment for H (Lecture 04), the CI photoionization cross section does not have a simple form, nor does the radiation field in the pertinent wavelength band from the IP of C to the IP of H: 11.26-13.60 eV or 912-1000A. Here are the facts:

$$\sigma_{\rm phion}({\rm C}) \approx 1.5{\rm x}10^{-17}{\rm cm}^{-2} \quad - \quad \text{mean value at } 1000 \text{ Å}$$

$$F_{\rm photon} = 2{\rm x}10^{7}{\rm cm}^{-2}{\rm s}^{-1} \quad - \quad \text{mean ISM UV photon flux at } 1000 \text{ Å}$$

The ISM/FUV is deduced from a 1968 calculation by Habing of the radiation field near the Sun from early type stars in the extreme FUV band from 950 - 1165 A. Draine uses 1.75 times this value. There is uncertainty on how the FUV flux vanishes at the Lyman limit.

Short Table of Ionization Potentials (eV)

Atom	Z	IP I	IP II	IP($1s^2$)	Ion
H	1	13.6			H I
He	2	24.6	54.4	24.6	He I
C	6	11.3	24.4	393	C V
N	7	14.5	29.6	552	N VI
O	8	13.6	35.1	739	O VII
Ne	10	21.6	41.0	1,196	Ne IX
Ar	18	15.8	27.7	4,121	Ar XVII
Fe	26	7.90	16.2	8,828	Fe XXV

Last two columns refer to the K-shell. The 1st IPs of Si, Mg and S are 8.15, 7.65 and 10.36 eV, respectively.

Photoelectric Heating of CI

With these data, we can calculate the photoionization rate:

$$G(\mathrm{C}) = \; F_{\mathrm{photon}} \mathrm{x} \sigma_{\mathrm{phion}}(\mathrm{C}) \approx 2\mathrm{x}10^{7}\,\mathrm{cm}^{-2}\mathrm{s}^{-1}\mathrm{x}\; 1.5\mathrm{x}10^{-17}\,\mathrm{cm}^{-2} = 1.8\mathrm{x}10^{-10}\,\mathrm{s}^{-1}$$

After multiplying by the abundance of carbon,2.5x10^{-4}, this rate is 1000 larger than the cosmic ray ionization rate. However, most carbon is in C^{+} in diffuse regions unshielded from ISM/FUV

Finally, we can estimate the heating by multiplying by the mean photo-electron energy, which we estimate as 1/2 of the interval from 10.26 to13.60 V, or 1.2 eV:

$$\Gamma(\mathrm{C}) = \; \Gamma(\mathrm{C})\; \Delta E(\mathrm{C}) n(\mathrm{C}) \approx 1.8\mathrm{x}10^{-10}\,\mathrm{s}^{-1}\;\mathrm{x}\; 1.2\mathrm{eV}\;\mathrm{x}\; 1.6x10^{-12}\,\mathrm{erg/eV}$$

or

$$\Gamma(\mathrm{C}) = 3.5\mathrm{x}10^{-26} \left(\frac{x(\mathrm{C})}{10^{-4}} \right) n_{\mathrm{H}}\ \mathrm{erg/s}$$

When account is taken of the fact that x(C) << x(C^{+}), photoelectric heating of C is comparable to cosmic ray heating, I.e., it Is weak. We can see this by looking at slide 16 for C^{+} cooling, whose numerical pre-factor will then be at least an order of magnitude larger and has a quadratic dependence on density.

Photoelectric Heating from Dust Grains

Atomic photoelectric heating is weak in diffuse neutral regions because some abundant ions (N, O, Ne) have IPs > 13.6 eV and those with IP < 13.6 eV, are easily ionized, resulting in low neutral atom abundances susceptible to photoionization by FUV radiation.

Grains and large molecules help solve this problem because they have IP < 13.6 eV and because they incorporate many heavy atoms including oxygen, with IP(O) > 13.6 eV (Lecture 06).

Treating photoelectric heating by grains and PAHs present technical issues, and we only summarize some of the important ones here.

Dust Grains: Size and charge are crucial

The mean free path for the liberated electron is much less than for the absorption of the UV photon. Photoelectrons generated in large grains (> 100 Å) are absorbed inside the grain and can't heat the gas. On the other hand, small grains are easily charged by the Interstellar radiation field, so that some of the energy of the photo-electrons is lost in overcoming the Coulomb potential of the grain.

Photoelectric Heating from PAHs

PAHS: Charge state is crucial

Like atoms, PAH molecules tend to have large second IPs, so only neutral PAHs lead to gas heating. Fortunately, their fraction Is substantial. The total abundance of PAHS then becomes important. Modeling of the PAH feature indicate that somewhere between 1-5% of all carbon is tied up in PAHS, for a PAH number fraction of ~ 10^{-7}. This is not such a small number relative to the fraction of carbon in neutral atomic form.

Calculations of photoelectric heating by small dust grains and large molecules indicate that the two are the same order of magnitude and are ~ 1000 times more effective than photoelectric heating of CI.

4. Ionization

Three basic methods for ionizing the gas are;

1. **External ionizing radiation (UV & X-rays)**
2. **Cosmic rays**
3. **Energetic gas kinetic collisions**

Cosmic rays are important only in cool radiation-shielded regions of interstellar clouds. Otherwise the main processes are ***radiative and collisional ionization.***

The role of collisional ionization for ion X depends on the ratio of $k_B T$ to the ionization potential IP(X). In this context, keep in mind these basic conversion factors:

$$k_B T = \frac{T}{11{,}605} eV \qquad \frac{ch}{\lambda} = 12{,}397 eV \left(\frac{A}{\lambda}\right)$$

Collisional Ionization of Heavy Ions

Cross sections for electronic ionization are generally much larger than for photoionization, but they are much harder to calculate (even for H) *and* to measure, at least for the moderate energies (1-100 eV) of astrophysical interest.

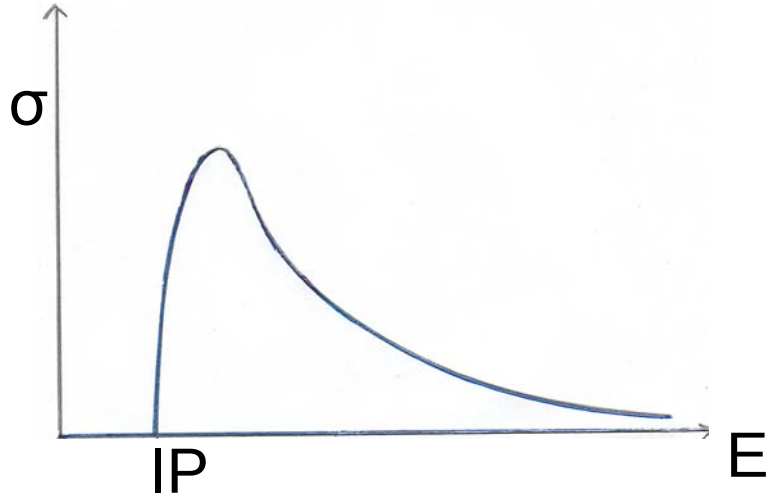

Useful reference for ionization cross sections: GS Voronov Atomic Data Nuclear Data Tables ATNDT 65 1 1997

Standard shape of an electronic ionization or excitation cross section after Bethe.

Collisional Ionization Models

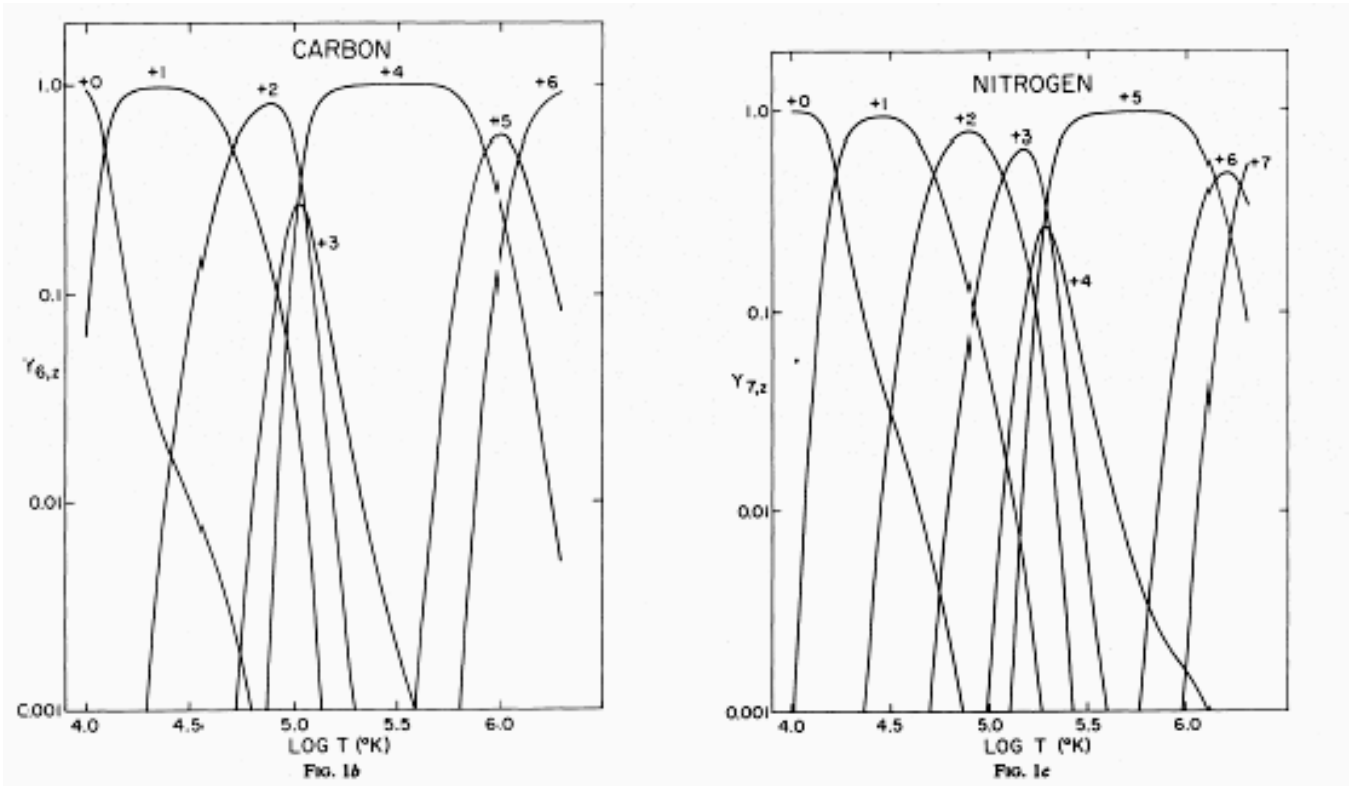

Fig. 1b Fig. 1c

Fractional abundance of ionization stage vs. *T*.

Shapiro & Moore ApJ 207 460 1976

Classic calculation of steady balance of collisional ionization and recombination for $T = 10^4$ - 5×10^6K.

Updated Collisional Ionization Model

RS Sutherland & MA Dopita, ApJS 88 353 1993, noteworthy for a good discussion of the underlying physics.

In addition to radiative and collisional ionization, a potentially critical reaction is **charge exchange**, e.g.,

$$H + A^{n+} \rightarrow A^{(n-1)+} + H^{+}$$

This reaction is very fast (rate coefficient 10^{-9} $cm^3 s^{-1}$ for large n, but is often slow for n = 1, 2. Rate coefficients for low-energy (< 1 eV) charge exchange are poorly known, except in special cases.

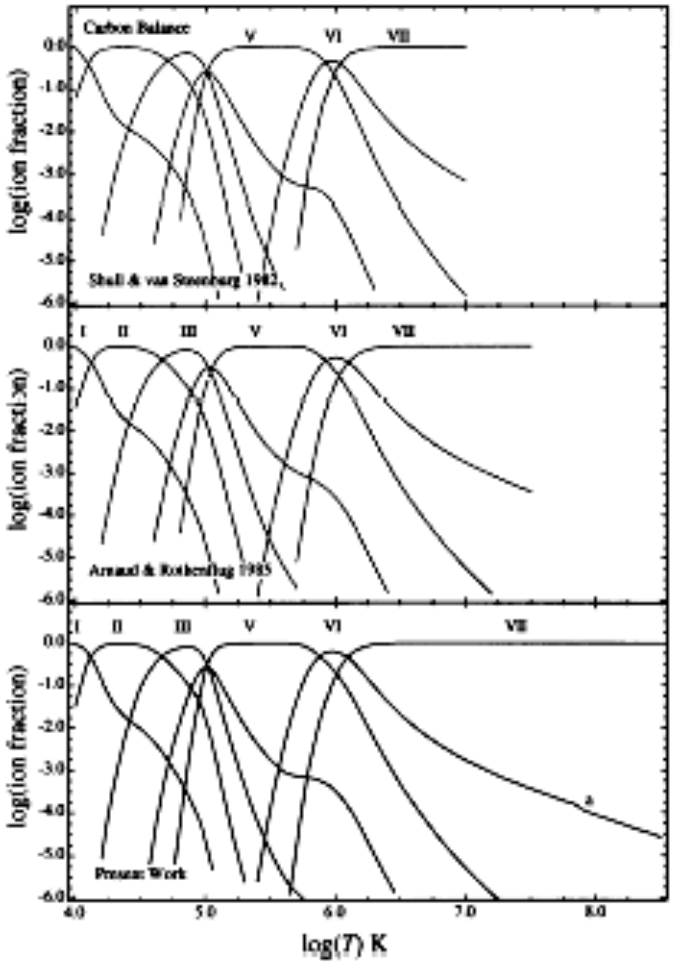

FIG. 3.—CIE balance for carbon. The results of Shull & van Steenberg (1982) (*upper panel*), Arnaud & Rothenflug (1985) (*center*), and MAPPINGS II (*lower panel*) curves. The extended hydrogenic recombination treatment allows the temperature range to be extended. The slight bump at (a) occurs at the change over to eqs. (19)–(22).

Ionization stage vs. *T*

Appendix A. Charge Exchange for O^+

Electronic recombination is a slow process, e.g., from Lecture 03

$$\alpha_2\,(8{,}000\mathrm{K},\ \mathrm{H}) = 3 \times 10^{-13}\ \mathrm{cm}^3\ \mathrm{s}^{-1}.$$

Particle reactions are often many orders of magnitude stronger, e.g., *fast* charge exchange of an ion and an *abundant* neutral is more important than recombination with electrons.

Perhaps the most important example for cool & warm regions is the *near-resonant* (and atypical) process

$$O^+ + H \longrightarrow H^+ + O \qquad \text{(exothermic)}$$

$$H^+ + O \longrightarrow O^+ + H \qquad \text{(endothermic)}$$

But the IP difference between O and H, 0.020 eV, is ~ same as the fine-structure splitting of the O ground state:

Fine Structure Levels of OI

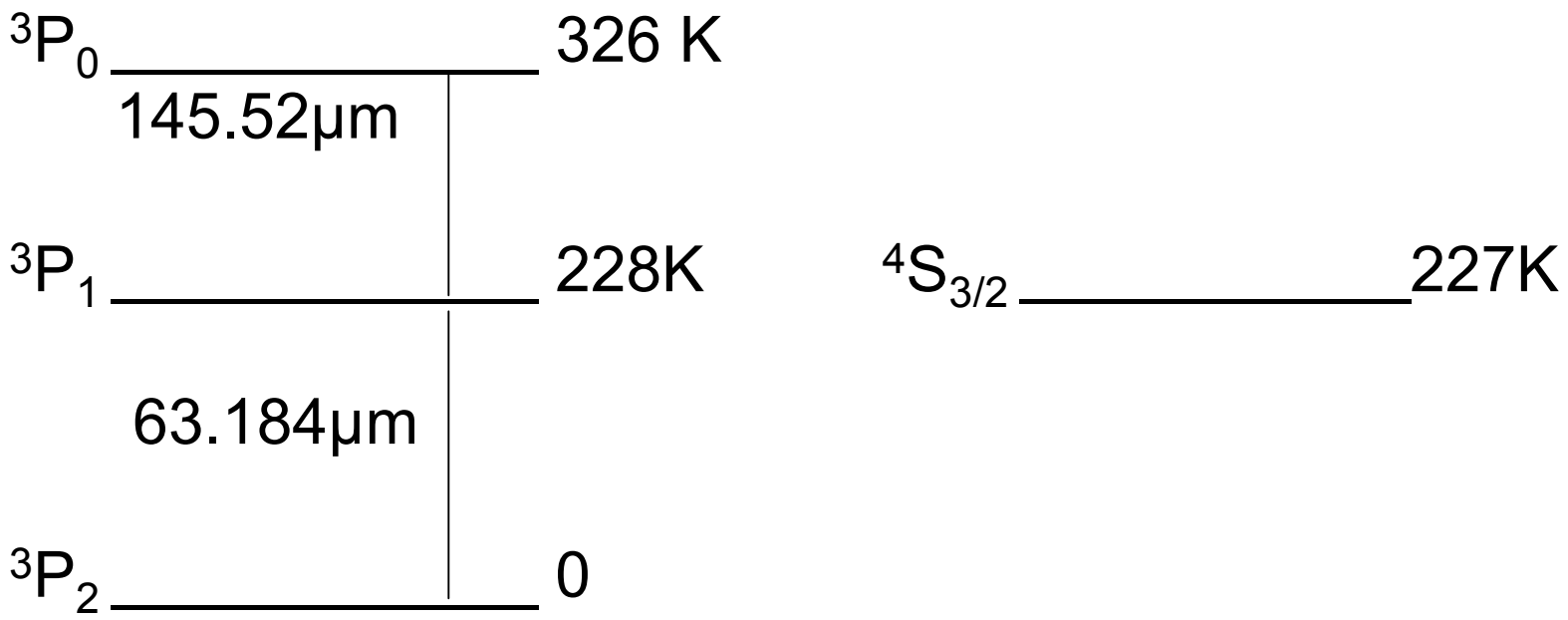

O (+ H^+)

Σ g = 9

O^+ (+ H)

Σ g = 4 x 2 = 8

g = statistical weight

The O^+/O Ratio

For T >> 300K, the exponential in the Milne relation between the forward (exothermic) and backward (endothermic) reactions is ~ unity; only the statistical weights matter:

$$k(H^+ + O) = (9/8)\ k(O^+ + H) \quad (\ T\ >> 300K\ ).$$

If O^+ is only produced and destroyed by charge-exchange reactions, steady balance reads:

$$k(H^+ + O)\ n(H^+)\ n(O) = k(O^+ + H)\ n(O+)\ n(H)\ .$$

Therefore the O/O^+ ratio is the H^+/H ratio multiplied by the ratio of rate coefficients:

$$\frac{n(O^+)}{n(O)} = \frac{k(H + O^+)}{k(O^+ + H)}\ \frac{n(H^+)}{n(H)} \rightarrow \frac{9}{8}\frac{n(H^+)}{n(H)} \quad (T >> 300K)$$

Definitive Calculation of O^+ + H Charge Exchange

Note different scales in upper & lower panels

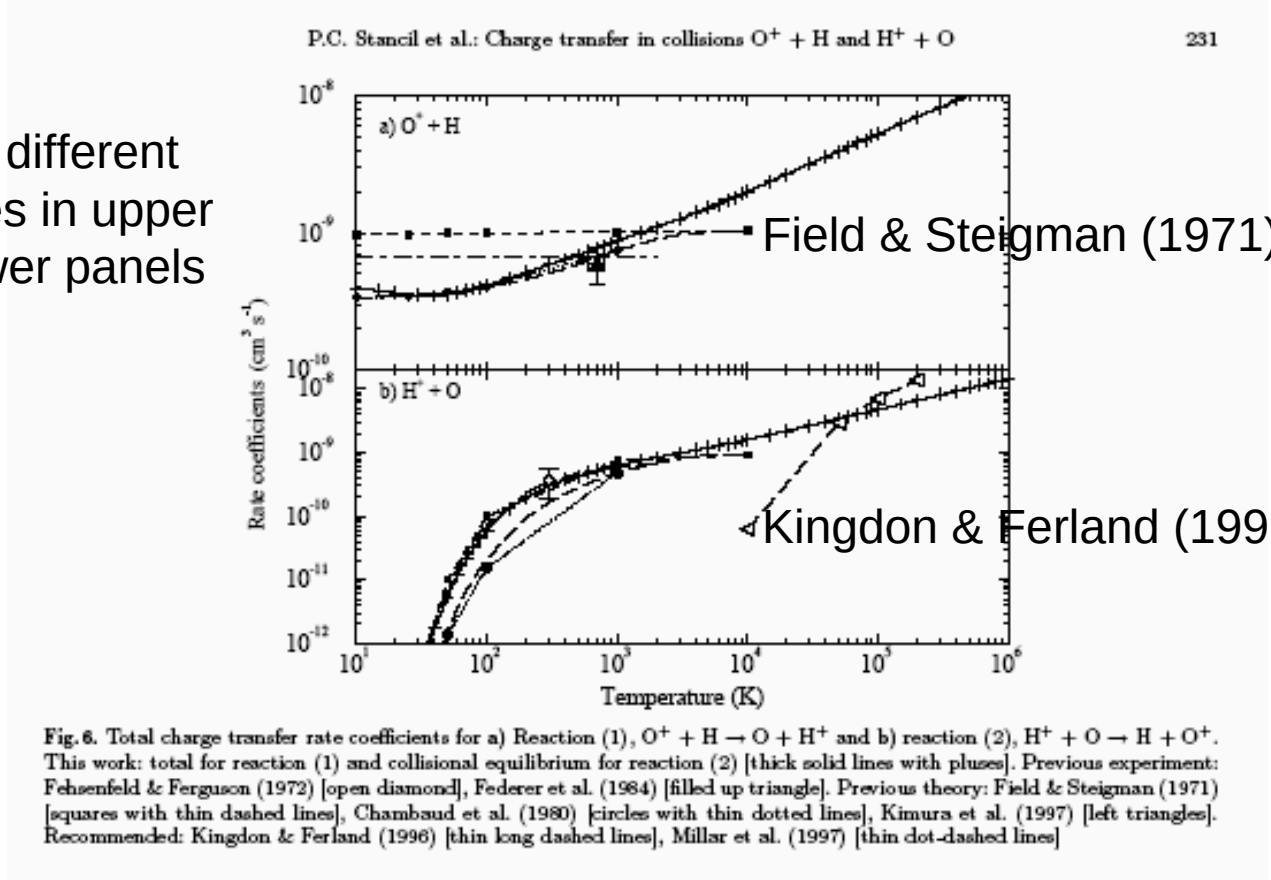

Fig. 6. Total charge transfer rate coefficients for a) Reaction (1), $O^+ + H \rightarrow O + H^+$ and b) reaction (2), $H^+ + O \rightarrow H + O^+$. This work: total for reaction (1) and collisional equilibrium for reaction (2) [thick solid lines with pluses]. Previous experiment: Fehsenfeld & Ferguson (1972) [open diamond], Federer et al. (1984) [filled up triangle]. Previous theory: Field & Steigman (1971) [squares with thin dashed lines], Chambaud et al. (1980) [circles with thin dotted lines], Kimura et al. (1997) [left triangles]. Recommended: Kingdon & Ferland (1996) [thin long dashed lines], Millar et al. (1997) [thin dot-dashed lines]

PC Stancil et al. A&AS 140 225 1999

There are large deviations from the 9/8 ratio below 300 K.

Appendix B. Dielectronic Recombination

Rather than making a direct radiative transition on capture,

$$e + A^+ \longrightarrow A^* + h\nu,$$

a doubly-excited configuration A** my be formed before radiating

$$\boxed{e + A^+ \longrightarrow A^{**} \longrightarrow A^* + h\nu}$$

a process known as ***dielectronic recombination***. It is more important than pure radiative recombination above 10.000-20,000K. A** can also re-emit an electron (auto-ionization), but then this is not recombination.

Reference on new calculations of recombination including radiative and dielectronic recombination:

Badnell, ApJS, 167, 334, 2006.

Older calculations:

Pequinot et al. A&A 251 680 1991

Landini & Monsignori-Fossi A&AS 91 193 1991

Comparison of New and Old Calculations
of Electronic Recombination Coefficients

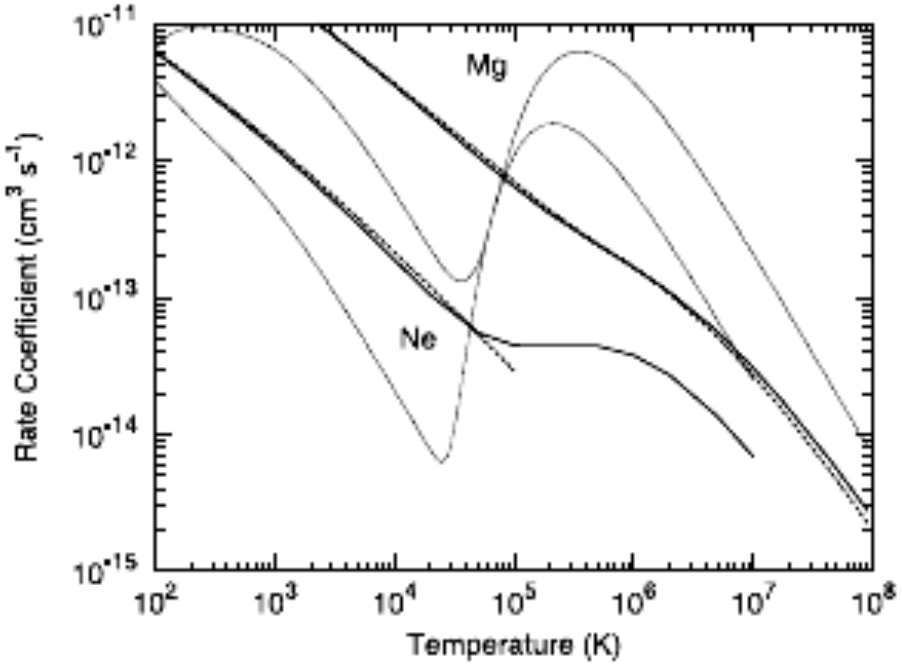

FIG. 6.—Total ground state rate coefficients for F-like Ne and Mg. *Solid curves*, present AUTOSTRUCTURE RR results; *dashed curves*, RR results of Péquignot et al. (1991) and Gu (2003) for Ne and Mg, respectively; *dotted curves*, DR results of Zatsarinny et al. (2006).

N.R. Badnell, ApJ 167, 334, 2006

Modern calculations: heavy lines

Older calculations: light iines